



Portable x-ray fluorescence as a tool for assessing electric marks in forensic evaluation

Stefano Tambuzzi¹  | Letizia Bonizzoni²  | Francesco Di Paola¹ |
Debora Mazzarelli¹ | Giulia Caccia¹ | Cristina Cattaneo¹

¹Department of Biomedical Sciences for Health, Institute of Forensic Medicine, University of Milan, Milan, Italy

²Department of Physics Aldo Pontremoli, University of Milan, Milan, Italy

Correspondence

Letizia Bonizzoni, Department of Physics Aldo Pontremoli, University of Milan, Celoria street, 16, 20133 Milan, Italy.
Email: letizia.bonizzoni@mi.infn.it

[Correction added on 7 August 2023, Some of the first and last names of the authors were mistakenly interchanged and have been corrected in this version.]

Abstract

Portable x-ray fluorescence (XRF) is a reliable, rapid and noninvasive technique. Recently, it has been used in a wide variety of fields where the sample must still be available after examination or when qualitative information on chemical composition is needed quickly to perform more detailed studies. These properties also make it suitable for forensic investigations, as shown by some recent reports. In the present work, a systematic evaluation of metal micro traces in electric marks was performed in a case of death by electrocution (high-voltage current). The results are promising, as XRF has been shown to be a suitable tool not only for skin fragments but also for graphite adhesive tapes placed on the body skin areas of forensic interest and then analyzed. The latter finding proves that skin samples at autopsy are not the only valuable sampling method, thus paving the way for the application of XRF in the diagnosis of electrical injuries in living individuals as well.

KEYWORDS

electrocution, forensics, high-voltage electrical marks, nondestructive analysis, XRF

1 | INTRODUCTION

Electrical injuries are a relatively rare but potentially devastating form of multisystem injury with high morbidity and mortality.¹ Electrocution occurs when an electric current passes through biological tissue: the damaging effects can result from both the heating due to the Joule effect of current passage and the direct action of the electric force on the charged or electrically polarized components of the tissue itself.² These damaged areas, known as electric marks, are usually circular or oval, dull yellow, hard and dry, and characterized by a palisade-like appearance of the epidermal cell nuclei; that means that these nuclei stretch and narrow to be arranged in the direction of

electric current.³ Evidence of electric marks plays a critical role in forensic evaluation, and the diagnosis of death by electrocution is based primarily on their morphological features in addition to field examination, case history, and histopathology.^{1,4} It is worth noting that only approximately one-third of electric shock death cases have a typical electric mark,⁵ which complicates the forensic diagnosis. In addition, autopsy examination of an electrocution victim often fails to reveal specific signs of the cause of death. Histochemical analyses (Pearl's reaction and rubeanic acid staining) of the skin can, however, reveal the metal traces that characterize this particular lesion,⁶ thus demonstrating metallization of the skin after electrical injury. Indeed, the Joule's heating effect and

This is an open access article under the terms of the [Creative Commons Attribution](https://creativecommons.org/licenses/by/4.0/) License, which permits use, distribution and reproduction in any medium, provided the original work is properly cited.

© 2023 The Authors. *X-Ray Spectrometry* published by John Wiley & Sons Ltd.

electrolysis caused by the passage of electric current through the body result in the deposition of metal ions. The chemical atoms involved in this process come from the electrodes, mainly iron and copper, but can vary depending on the metal alloy. Previous work in the forensic field had proven that fine particles of metal elements from the surface of the electrical conductor are deposited in the injured skin due to the effects of high temperature and electric field during electrocution, even when no current marks on the skin were evident.^{7,8} Their successful detection is, therefore, of enormous importance from a forensic point of view. In addition to histological staining techniques,^{7,9} more technologically advanced methods are used to detect metallization of the skin, including atomic absorption spectroscopy (AAS)^{10,11} and scanning electron microscopy with energy dispersive x-rays (SEM/EDX).¹² The latter has proven useful in forensics to successfully detect micro traces of Cu and Zn, as well as Fe and Cr in electric marks.^{9,13,14} SEM/EDX, however, remains underused due to its high cost, long investigation time, and the high level of expertise required to correctly interpret the results. In addition, SEM/EDX does not preserve the sample, unlike x-ray spectrometry (XRF) technology, which has simpler performance, repeatability, and lower cost. Several aspects suggest that XRF could be a good candidate for forensic applications compared to SEM/EDX: (1) no need to examine samples in a vacuum chamber, simpler sample preparation, and generally easier to perform; (2) lower cost; (3) repeatability due to unaltered sample preservation; (4) faster procedure; (5) higher sensitivity for heavier elements; (6) deeper penetration of x-ray beam than electron beam; (7) higher peak resolution; (8) better detection limit allowing identification of multiple trace elements; (9) possibility to use portable equipment.^{15,16} Despite all this, the use of XRF has been proposed only in one forensic case where it was possible to correctly assess a suspected electrical death.¹⁷ In recent reports,^{18,19} XRF has proven to be a good technique for various forensic investigations, including analyses of human remains.^{20–22} Its potential applications in forensic practice can be very useful anytime a medium-high Z element has to be detected in a light matrix, as reported by several applications in other fields.^{23–26}

Given this great versatility and enormous potential, we experimentally used a portable XRF spectrometer in a real forensic case in which a man died from a high-voltage electric shock. We then performed a systematic assessment of metallic micro traces in electric marks in different skin fragments sampled at autopsy, as well as on graphite adhesive tapes placed on the body skin areas of forensic interest. This innovative investigation was intended to test whether it is only possible to work directly on cadaveric skin or whether this approach could

be overcome. If so, this would open up the important frontiers of applying XRF technology on living individuals, such as victims of torture by electric shock. This phenomenon is well described in the literature, with incidence ranging from 8% to 24% depending on the country of origin.^{27–31} Overall, the goal was to expand current knowledge of XRF in assessing electric marks and evaluate new applications in forensics.

2 | MATERIALS AND METHODS

2.1 | Sampling procedures

The case involved a man who was found dead on the electrified tracks of a city subway. The prosecutor ordered a judicial autopsy to determine the manner and cause of death. Because several areas of skin with macroscopic electric marks were noted at autopsy, XRF analysis was performed to assess the metallization of the skin. The likelihood that the man died from electrocution was very high because the subway line in question was electrified at 750 V DC via a third side rail system and used an additional central fourth rail for grounding and negative electrical return. The rails of the track are made of high-quality steel. Typically, it is a hot-rolled steel with medium carbon content, about 98% of which is Fe. Carbon steels have C as the main alloying element; other elements include Mn (up to 1%), Si (up to 0.4%), P (about 0.05%), S (0.04%) and residual elements such as Ni, Cr, Al, Mo, and Cu; therefore, it was expected Fe to be deposited as a metallic element in the electric marks since the rail tracks served as electrodes.

To obtain a reliable XRF analysis looking for signs of electrical injury and skin metallization, the preliminary washing of the body before the autopsy was avoided to preserve any residual exogenous material. At autopsy, seven small skin fragments (approximately 1 cm × 1 cm × 0.5 cm) were excised from the electric marks using a knife with a ceramic blade. The use of such a tool was considered necessary to avoid possible contamination of the specimens by metallic micro traces originating from the blades of the autopsy instrumentation. The sampling sites were the posterior surface of the right thigh, the posterior surface of the left thigh, the second finger of the left hand, the ulnar surface of the left hand, the nape, the right scapula, and the left scapula. These sites have been reported in Table 1, accompanied by further details, including skin thickness and if they were covered with clothing items or not. A negative control skin sample was also collected from the abdomen, that is, from an injury-free area away from the electric marks. After sampling, all skin fragments were placed in histological boxes and put in 10% buffered

formalin. Examples of the nature and appearance of the collected samples are shown in Figure 1.

In addition, graphite adhesive tape was used as an alternative sampling method on a subset of the electric marks, corresponding to the posterior surface of the left thigh, the second finger of the left hand, the ulnar surface of the left hand, and the right scapula (Table 1). Graphite adhesive tape was positioned and pressed onto the damaged tissue that was in direct continuity with the areas that had been previously excised. The reason for this

choice was to apply the two methods to areas that were morphologically as similar as possible without altering the skin fragments before analysis or removing metal particles, which could happen if the sampled areas matched exactly. Negative control was collected by positioning and pressing the graphite adhesive tape onto the abdomen. All the tape pieces were fixed on microscope slides and were immediately placed in a hermetically sealed sterile tube to avoid potential environmental contamination.¹⁴

TABLE 1 List of specimens submitted for x-ray fluorescence analysis, accompanied by relevant further details (macroscopic skin features and presence of clothing).

Measure number	Body area	Skin fragment	Thickness	Graphite adhesive tape samples	Details
1	Posterior surface of right thigh	<input checked="" type="checkbox"/>			Covered by trousers
2	Posterior surface of left thigh	<input checked="" type="checkbox"/>		<input checked="" type="checkbox"/>	Covered by trousers
3	Second finger of left hand A	<input checked="" type="checkbox"/>	<input checked="" type="checkbox"/> (1 mm)		Including only epithelium. Visible charring
4	Second finger of left hand B	<input checked="" type="checkbox"/>	<input checked="" type="checkbox"/> (1 mm)	<input checked="" type="checkbox"/>	Including only epithelium. No visible charring
5	Ulnar surface of left hand	<input checked="" type="checkbox"/>	<input checked="" type="checkbox"/> (4 mm)	<input checked="" type="checkbox"/>	Including the subcutaneous fat layer
6	Nape A	<input checked="" type="checkbox"/>			Preserved hair
7	Nape B	<input checked="" type="checkbox"/>			Charred hair
8	Right scapula	<input checked="" type="checkbox"/>		<input checked="" type="checkbox"/>	Covered by shirt
9	Left scapula	<input checked="" type="checkbox"/>	<input checked="" type="checkbox"/> (6 mm)		Overlying torn shirt
10	Abdomen	<input checked="" type="checkbox"/>	<input checked="" type="checkbox"/> (5 mm)	<input checked="" type="checkbox"/>	Negative control (injury-free skin area)

Note: Thickness is given only for samples where the inner surface has also been analyzed by irradiation.



FIGURE 1 Examples of skin fragments collected from some electric marks (nos. 6 and 9) and the negative control skin sample (no. 10). [Colour figure can be viewed at wileyonlinelibrary.com]

2.2 | XRF analysis

For the analysis of the selected skin samples, the home-made spectrometer FUXYA2020³² was used, which mounts a MINI-X2 x-ray tube (Amptek, Bedford, MA) with a maximum power of 4 W (50 kV, 200 μ A) and a transmission rhodium anode. The x-ray tube is coupled to an SDD XGL-SPCM-DANTE-25 detector (XGLAB Bruker Nano Analytics), with a nominal energy resolution of 130 eV at 5.9 keV for operating conditions. The working conditions of the XRF spectrometer for the measurements reported in this work were 50 kV and 0.4 mA with an acquisition time of 30 s.

The collected skin samples were removed from the formalin and briefly rinsed with pure water to remove formalin and particulate residues that could contaminate the samples. They were then analyzed. A total of 9 acquisitions were performed on the different skin samples, as shown in Table 1. In addition, also the negative control sample (hereafter sample no. 10) was analyzed. The number of XRF measurements exceeds the number of fragments by two, because two different spots were assessed for two of them, namely the left second finger (sample nos. 3 and 4) and the nape (sample nos. 6 and 7). XRF analysis of the inner surface was also performed on some specimens (nos. 3, 4, 5, 9, and 10) to investigate the penetration of the metallization into the skin.

Graphite adhesive tape samples were analyzed with the same spectrometer. Since they had been mounted on microscope slides prior to analysis, it was deemed necessary to also perform XRF analysis on a blank slide to distinguish the elements present in the samples taken from the body from those in the glass slides. The negative control sample (sample no. 10) was also assessed.

It was decided not to perform any quantitative analysis of Fe content because the sample surface was very irregular, and it was not possible to define areas or depths to be studied: this would have resulted in unreliable quantification without any information other than the qualitative assessment reported in this article. For this reason, no minimum detection limit is reported, but a semi-quantitative assessment was performed using undamaged skin (negative control sample) as a reference for average Fe content.

2.3 | Ethical approval

The subject involved in this study underwent a judicial autopsy at the Institute of Forensic Medicine of Milan in order to identify the cause of death. Data collecting, sampling, and subsequent forensic analysis were authorized by the public prosecutor. Therefore, data were acquired

as part of a forensic judicial investigation and in accordance with the Italian Police Mortuary Regulation. Consequently, in accordance with Italian law, ethical approval was not required in these cases. Moreover, all the studies conducted followed the guidelines provided by Legislation and the National Bioethical Committee and guidelines by Helsinki Declaration. Publication of data is allowed when the case has been closed, but the anonymity of the subject must be guaranteed.

3 | RESULTS

3.1 | Results on skin fragments

The comparison between XRF spectra obtained on skin fragments of the ulnar surface of the left hand, left scapula, and negative control is shown in Figure 2. As expected, the main difference is in the intensity of Fe peaks since this element was the main component of the rail tracks that served as electrodes in the present case. The reported spectra are normalized to the intensity of the Rayleigh peak of the Rh (tube anode) $K\alpha$ line and then shifted for clarity. From the relative intensity of the Compton scattered peak of the Rh $K\alpha$ line, a slightly higher average Z can be inferred for the samples collected from the electric marks, indicating metallization of the skin; the slightly different position of the Rh- $K\alpha$ -Compton scattering peak is instead related to the possibly different geometry of the examined skin fragments. It is also interesting to note that Mn signals, which are related to the chemical composition of the steel that makes up the rail tracks, are barely visible in the spectrum of the left-hand skin, while the Fe peaks are very high (Figure 2).

Traces of Ca, Ti, Fe, Cu, and Zn were detected in the negative control. Results for the other skin fragments are summarized in Table 2. For each sample, only those elements not present or present in higher amounts than in the negative control (sample no. 10) have been indicated in the “other elements” column. For Fe, the ratio between the $K\alpha$ peak and the Rayleigh scattering peak of Rh was considered; the peak areas were calculated by fitting the spectra and subtracting the background in the region of interest. Since Rh is the element that makes up the transmission anode of the x-ray tube, its signal is ubiquitous in the incident beam, and the Fe/Rh ratio can serve as a parameter to normalize the different Fe measurements, compensating for possible geometric heterogeneities in the samples (i.e., size, shape, and thickness) and minimal variations in the sample distance from the source. The choice of Fe as a marker element is the direct consequence of the composition of the rail tracks (about

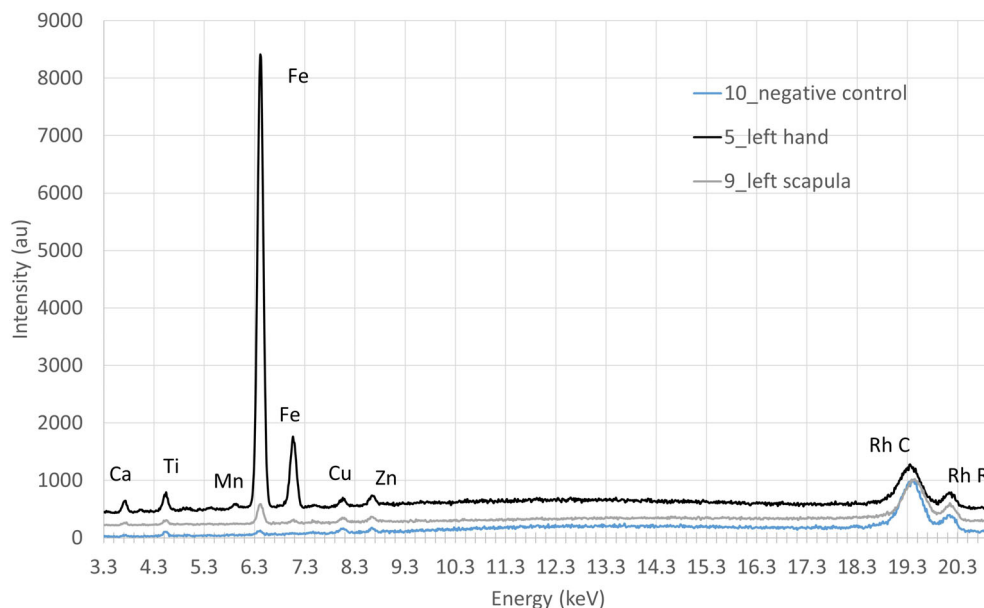


FIGURE 2 Comparison of x-ray fluorescence spectra of skin fragments from the ulnar surface of the left hand, left scapula, and negative control. [Colour figure can be viewed at [wileyonlinelibrary.com](https://onlinelibrary.wiley.com)]

TABLE 2 Results of x-ray fluorescence (XRF) analysis of skin fragments and graphite tape samples; trace elements are reported in brackets.

XRF measure	Skin sample analysis outer surface irradiation		Skin sample analysis inner surface irradiation	Graphite tape analysis
	Other elements	Fe/Rh	Fe/Rh	Fe/Rh
1	Ti	0.2		
2		0.3		0.4
3	Ca, Ti	7.8	7.7	
4	Fe	0.4	0.8	0.7
5	Ca, Ti, Mn, Cu, Zn (Cr)	9.6	0.1	1
6	Fe	0.3		
7	Fe	0.3		
8	(Br)	0.2		0.8
9		0.6	0.1	
10		0.2	0.1	0.5

98% Fe concentration in the alloy). The negative control for skin fragments gave a Fe/Rh ratio of 0.2. Considering this ratio as a threshold indicator of electrical metallization, even without visible traces, it can be seen that no micro traces of iron were found in samples 1, 2, and 8, where the skin was covered with clothing. All other electric marks were characterized by an increased peak area of iron signals, even if there was no visible charring, for instance, in sample no. 4. In the cases where the iron content was much higher (sample no. 5), a number of other elements could also be detected, while sample 8 showed traces of bromine (Table 2).

Figure 3 shows the comparison between the XRF spectra of skin fragments of the second finger of the left

hand B (sample no. 4) when irradiated from the outer and inner surfaces. As can be seen, the Ca signals are less intense, while the Fe peaks are almost comparable to those obtained when irradiating the outer surface. Compared with the results obtained from irradiation of the inner surface of sample 10 (negative control), the XRF analyses of the inner surface of sample nos. 3 and no. 4, – both performed on the second finger of the left hand, mirror the results obtained from irradiation of the outer surface, as can be seen from the ratios given in Table 2. Sample nos. 5 and no. 9, the thickest ones, showed no discernible differences from the XRF analysis of the inner surface of skin reference sample no. 10 (see Table 2).

3.2 | Results on graphite adhesive tape samples

The blank glass slide (sample no. 0) contained Ca and As and traces of K, Cu, Zn, Se, Rb, and Zr, all elements of no interest to our research. The negative control (sample no. 10) showed the presence of elements from the slide itself with the addition of very small traces of Ti and Fe. In addition, the Ca signal from the slide was partially absorbed by the tape due to its relatively low energy, unlike the As signal. For each sample, no elements were detected except Fe and the elements in the blank and the negative control samples. As expected, some of the tape samples showed an increase in Fe peak intensity. In detail, Figure 4 shows the comparison between the

negative control (sample no. 10) and the ulnar surface of the left hand (sample no. 5). The spectra given are normalized to the intensity of the Rayleigh peak of the Rh (tube anode) $K\alpha$ line and then shifted for clarity. As with the skin fragments, the Fe/Rh ratio was considered, resulting in a value of 0.5 for the negative control sample, which was therefore considered a threshold for positive metallization. The results for the graphite adhesive tape samples are summarized in Table 2.

4 | DISCUSSION

As shown in Table 2, no Fe micro traces were detected in sample nos. 1, no. 2, and 8, where the skin was covered

FIGURE 3 Comparison between x-ray fluorescence spectra of skin fragments from the second finger of the left hand B, following irradiation from the outer and inner surfaces.

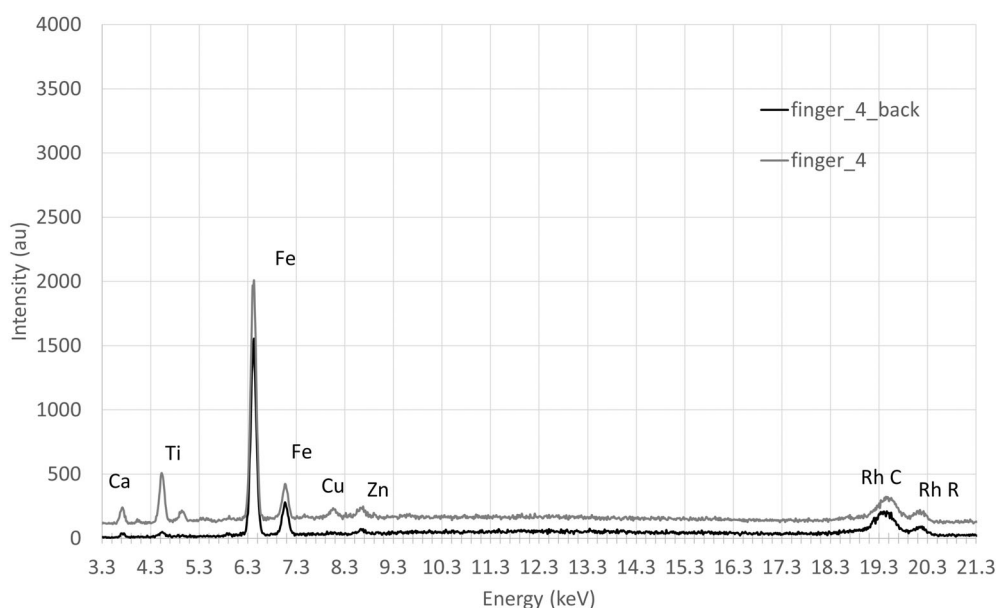
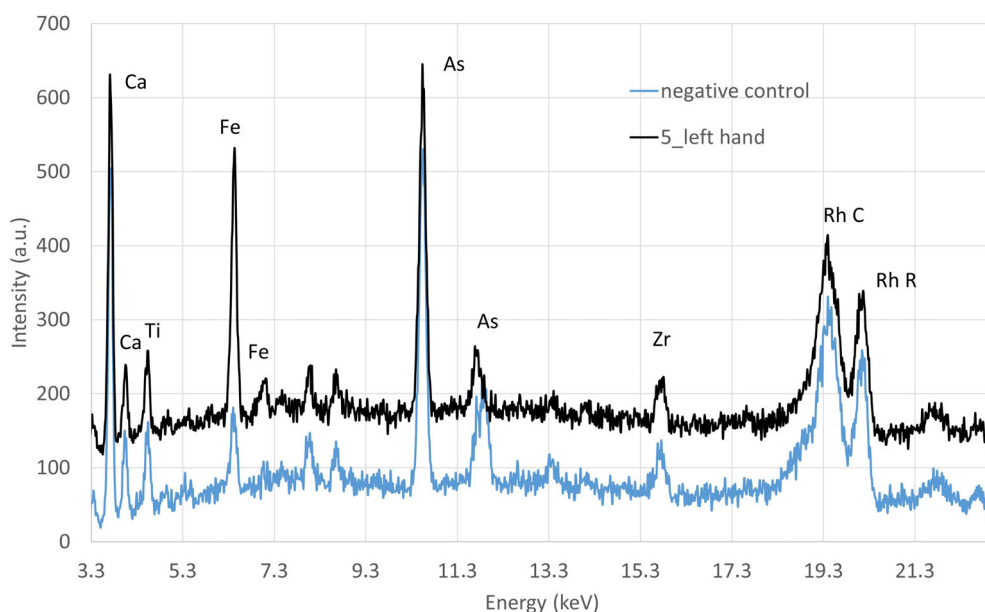


FIGURE 4 Comparison between x-ray fluorescence spectra of graphite adhesive tape samples of the ulnar surface of the left hand and the negative control. [Colour figure can be viewed at wileyonlinelibrary.com]



with clothing. All other electric marks, where clothing was absent or torn (as in sample no. 9), were characterized by an increased peak area of Fe signals, even when (as in sample no. 4) there was no visible charring. In the cases where the Fe content was much higher (sample no. 5), other elements could also be detected (Ca, Ti, Mn, Zn, Cu, and traces of Cr), which may be minor components of the steel rail tracks that served as the electrode. The presence of Br in sample 8 may be due to the presence of a shirt over the skin. Indeed, organobromine flame retardants are used in the textile industry.³³ Therefore, it can be reasonably concluded that the presence of garments can prevent the metallization of the skin or bring it to a value below the detectability threshold.

In this study, it was also attempted to obtain information on the depth of penetration of the metallization into the skin, but XRF on skin samples gave no definite answer. For this purpose, the inner surface of the skin samples was also analyzed, but to correctly evaluate the results reported in Table 2, it was necessary to consider the possibility that Fe from the outer surface may be excited by radiation penetrating into the inner surface of the skin samples. Specifically, the expected absorption of the Fe signal from the outer surface of the sample caused by the thickness of the samples was calculated. The absorption coefficient of the skin fragments was approximated to that of polymethyl methacrylate (PMMA), an engineering plastic with a density of 1.19 g/cm³ commonly used as a soft tissue substitute for diagnostic imaging. Since the mass attenuation coefficient μ/ρ for the Fe-K α line (6.4 KeV) is 12.71 cm²/g, the Beer–Lambert law can be used to calculate the expected signal absorption/transmission for the analyzed specimens: sample nos. 3 and no. 4 (second finger of the left hand) have a thickness of 1 mm, resulting in an absorption of 78%; sample no. 5 (ulnar surface of the left hand) has a thickness of 4 mm, with an absorption of about 99%; sample no. 9 (left scapula) has a thickness of 6 mm with an absorption of more than 99%. For thicker samples with higher absorption, if any Fe signal was detected after irradiating the inner surface of the skin fragment, it was not possible to exclude the influence of Fe on the outer surface; however, for these samples, the results in Table 2 show that there was no Fe increase compared with the skin reference sample (inner irradiation measurement). This indicates that the penetration of the metal particles into the epithelial tissue was less than 4 mm. When a significant Fe signal was detected in the analysis of the inner surface of a sample, as was the case with sample no. 3, among the thinnest samples examined, particular attention had to be given to the possible transmission of Fe signals from the outer surface. If the Fe peak originated from Fe particles on the outer skin surface, one would expect to detect a Fe peak about 78% less intense

than that detected by irradiating the outer skin surface. Based on the peak areas of the spectra shown in Figure 3, the intensity of the Fe peak after irradiating the sample from the inner surface was, however, only about 20% less intense. We can, therefore, assume that the metallization penetrates into the skin and rule out a deposition of Fe particles limited to the surface, although it was not possible to calculate how deep the particle deposition in the epithelial was. A more reliable method to quantify the depth of skin metallization in a future study would be to use particle-induced x-ray emission (PIXE) instead of XRF spectroscopy. In this technique, the excitation beam consists of protons whose penetration depth into the samples is less than that of x-rays.³⁴

The results obtained with graphite tape samples were similar to those obtained with the skin samples, of course, with reference only to the outer surface analysis. In detail, sample nos. 4 and 5 allowed to detect an evaluable rise in Fe/Rh ratio, while the result obtained on sample no. 2 was not useful to detect the Fe increase. It is worth noting that for sample no. 8, the graphite tape sample proved to be even more effective than the fragment specimen. Although the two samples were collected from the same body region, they were not taken from the exact same location, so there may be differences in the degree of metallization that are not visible macroscopically; the same applies to sample no. 2. The effectiveness of the tape collection in detecting skin metallization is of utmost importance, as it proves that skin fragments from autopsies—or skin biopsies—are not the only valuable specimens for this purpose. Since graphite adhesive tape collection is a noninvasive method, it can be easily applied to living humans and not only to bodies. Further studies are needed because x-ray fluorescence spectroscopy has the potential to become a rapid, sensitive, and specific diagnostic test for electrocution in the dead and for electrical injury in the living. The most important case in which it is medically relevant to diagnose the occurrence of electrical trauma in a living subject is probably in the context of torture, since electrical torture accounts for hundreds of cases.^{27–30} Most examinations of torture victims take place months or years after the torture, and electrical torture often leaves barely perceptible or no traces, making the diagnosis extremely challenging.³¹ One technique sometimes used to detect electrical injury in a suspected torture victim is histopathology, but a number of studies have shown that x-ray microanalysis is more sensitive than histochemical methods, plus it is multielemental and does not necessarily require a skin biopsy.^{13,14,17} Another interesting point to be clarified is the duration of detectability of the metal particles by XRF spectroscopy. The diagnostic value of this method would be strengthened by possible future studies demonstrating the persistence of these elements

in the skin despite tissue renewal and exposure to shear forces, atmospheric agents, and detergents.

The literature on the use of XRF spectroscopy in forensics is limited, although it has several proven and potential advantages. Most importantly, XRF spectroscopy is completely nondestructive and does not consume the sample, which is particularly important because forensic samples are unique and often very small.^{15,16} In contrast, the literature on the use of SEM/EDX in forensics is extensive.¹⁴ By combining scanning electron microscopy and x-ray microanalysis, the latter has the undeniable advantage of simultaneously revealing the 3D microstructure of a sample and its chemical composition, whereas XRF spectroscopy only provides compositional information. Moreover, SEM/EDX is more sensitive than XRF to lighter elements, which are more abundant in organic and biological samples. Nevertheless, as stated in the introduction, XRF spectroscopy has some advantages over its “sister” technique. In addition, the wise use of comparative analysis of spectra can undoubtedly provide valuable data to forensic scientists. Therefore, there is undoubtedly a need for scientific work aimed at exploring the potential applications of this technique in samples of forensic interest. Future studies should focus on the application of XRF spectroscopy to other types of injuries, as particles invisible to the naked eye can also provide valuable information about weapons and perpetrators in cases of sharp and blunt injuries, gunshot wounds, and ligature strangulation.


5 | CONCLUSION

It is critical that physicists and professionals who study the working mechanisms of elemental analysis techniques such as XRF are aware of the extensive applications of these tools in the forensic field. Our analysis paved the way for future developments in the application of this technique to diagnose death by electrocution, as well as to detect electrical injury in the living, which is important both in the judicial setting and in the context of human rights violations. Indeed, this elemental analytical technique has the potential to be useful or even crucial in forensic investigations because it is multielemental, non-destructive, rapid, sensitive, and relatively inexpensive. From the results of our study, it is fair to conclude that XRF spectroscopy deserves a place in the arsenal of forensic pathologists and scientists.

DATA AVAILABILITY STATEMENT

The data that support the findings of this study are available from the corresponding author upon reasonable request.

ORCID

Stefano Tambuzzi  <https://orcid.org/0000-0003-4711-5545>

Letizia Bonizzoni  <https://orcid.org/0000-0002-8637-7006>

REFERENCES

- [1] X. Jin, D. Chen, X. Li, X. Zeng, L. Xu, B. Hu, G. Xu, *Int. J. Leg. Med.* **2021**, *135*, 2469.
- [2] A. Sanford, R. L. Gamelli, in *Handbook of Clinical Neurology*, Vol. 120 (Eds: J. Biller, J. M. Ferro), Elsevier, Amsterdam **2014**, p. 981.
- [3] E. Bellini, G. Gambassi, G. Nucci, M. Benvenuti, G. Landi, M. Gabbriellini, P. Vanezis, *Forensic Sci. Int.* **2016**, *264*, 24.
- [4] J. Gentges, C. Schieche, *Emerg. Med. Pract.* **2018**, *20*(11), 1.
- [5] G. Xu, R. Su, J. Lv, X. Lai, X. Li, J. Wu, B. Hu, L. Xu, R. Shen, J. Gu, X. Yu, *Int. J. Leg. Med.* **2017**, *131*, 433.
- [6] R. K. Wright, J. H. Davis, *J. Forensic Sci.* **1980**, *25*, 514.
- [7] H. Jacobsen, *Forensic Sci. Int.* **1997**, *90*, 85.
- [8] T. Marcinkowski, M. Pankowski, *Forensic Sci. Int.* **1980**, *16*, 1.
- [9] N. Tanaka, H. Kinoshita, M. Jamal, M. Kumihashi, K. Tsutsui, K. Ameno, *Leg. Med.* **2013**, *15*, 283.
- [10] K. Acar, B. Boz, A. Kurtulus, U. Divrikli, L. Elci, *Forensic Sci. Int.* **2004**, *146*, S3.
- [11] M. Jakubeniene, A. Zakaras, Z. N. Minkuviene, A. Benoshys, *Forensic Sci. Int.* **2006**, *161*, 36.
- [12] H. Kinoshita, M. Nishiguchi, H. Ouchi, T. Minami, A. Kubota, T. Utsumi, N. Sakamoto, N. Kashiwagi, K. Shinomiya, H. Tsuboi, S. Hishida, *Leg. Med.* **2004**, *6*, 55.
- [13] M. Boracchi, G. Domenico Luigi Crudele, G. Gentile, F. Maciocco, F. Maghin, M. Marchesi, E. Muccino, R. Zoja, *Med. Leg. J.* **2019**, *87*, 67.
- [14] G. Gentile, S. Andreola, P. Bailo, A. Battistini, M. Boracchi, S. Tambuzzi, R. Zoja, *Am. J. Forensic Med. Pathol.* **2020**, *41*, 280.
- [15] B. Beckhoff, B. Kanngießer, N. Langhoff, R. Wedell, H. Wolff, *Handbook of Practical X-Ray Fluorescence Analysis*, Springer Science & Business Media, Berlin **2007**.
- [16] K. Leopold, *Anal. Bioanal. Chem.* **2021**, *413*, 6455.
- [17] T. Wang, D. Zou, J. Zhang, Y. Chen, *Am. J. Forensic Med. Pathol.* **2016**, *37*, 190.
- [18] C. R. Appoloni, F. L. Melquiades, *Appl. Radiat. Isot.* **2014**, *85*, 92.
- [19] G. Vittiglio, S. Bichlmeier, P. Klinger, J. Heckel, W. Fuzhong, L. Vincze, K. Janssens, P. Engström, A. Rindby, K. Dietrich, D. Jembrih-Simbürger, M. Schreiner, D. Denis, A. Lakdar, A. Lamotte, *Nucl. Instrum. Methods Phys. Res., Sect. B* **2004**, *213*, 693.
- [20] J. K. Pringle, A. J. Jeffery, A. Ruffell, I. G. Stimpson, D. Pirrie, E. Bergslien, C. Madden, I. Oliver, K. D. Wisniewski, J. P. Cassella, N. Lamont, S. Gormley, J. Partridge, *Forensic Sci. Int.* **2022**, *332*, 111175.
- [21] J. F. Fonseca, M. M. Cruz, M. L. Carvalho, *X-Ray Spectrom.* **2014**, *43*, 49.
- [22] V. Merelli, G. Caccia, D. Mazzarelli, L. Franceschetti, O. Paciello, L. Bonizzoni, M. Caccianiga, C. Campobasso, C. Cattaneo, *Int. J. Leg. Med.* **2023**. <https://doi.org/10.1007/s00414-023-03021-1>
- [23] E. Marguí, I. Queralt, M. Hidalgo, *TrAC Trends Anal. Chem.* **2009**, *28*, 362.

- [24] K. E. Young, C. A. Evans, K. V. Hodges, J. E. Bleacher, T. G. Graff, *Appl. Geochem.* **2016**, *72*, 77.
- [25] L. Bonizzoni, A. Galli, G. Spinolo, V. Palanza, *Anal. Bioanal. Chem.* **2009**, *395*, 2021.
- [26] F. Micheletti, J. Orsilli, J. Melada, M. Gargano, N. Ludwig, L. Bonizzoni, *Microchem. J.* **2020**, *153*, 104388.
- [27] M. S. Pollanen, *Forensic Sci. Int.* **2018**, *284*, 85.
- [28] P. Perera, *J. Forensic Leg. Med.* **2007**, *14*, 146.
- [29] D. Forrest, *Forensic Sci. Int.* **1995**, *76*, 77.
- [30] R. Clément, D. Lebossé, L. Barrios, O. Rodat, *J. Forensic Leg. Med.* **2017**, *46*, 24.
- [31] B. Madea, *Handbook of Forensic Medicine*, John Wiley & Sons, Hoboken **2014**.
- [32] G. Ruschioni, F. Micheletti, L. Bonizzoni, J. Orsilli, A. Galli, *Appl. Sci.* **2022**, *12*, 3.
- [33] A. R. Horrocks, *Polymer* **2020**, *12*, 9.
- [34] N. Grassi, A. Migliori, P. A. Mandò, H. C. del Castillo, *X-Ray Spectrom.* **2005**, *34*, 306.

How to cite this article: S. Tambuzzi, L. Bonizzoni, F. Di Paola, D. Mazzarelli, G. Caccia, C. Cattaneo, *X-Ray Spectrom* **2024**, *53*(2), 112.
<https://doi.org/10.1002/xrs.3390>